8th International DAAAM Baltic Conference
"INDUSTRIAL ENGINEERING"
19-21 April 2012, Tallinn, Estonia

# OPTIMIZING AEROSOL JET® PRINTING OF SILVER INTERCONNECTS ON POLYIMIDE FILM FOR EMBEDDED ELECTRONICS APPLICATIONS

**Verheecke, W.; Van Dyck, M.; Vogeler, F.; Voet, A., Valkenaers, H.**

**Abstract:** *The Aerosol Jet® Printing (AJP) process is a fine feature sub-micron scale deposition process. The paper discusses the optimization of AJP in order to achieve the desired quality of printed silver ink interconnects on polyimide film for embedded electronics applications. A process window containing the parameters which have influence on the quality aspects of the printed tracks is determined to obtain the optimal quality. Important quality aspects in this research include the geometrical and electrical properties of the printed tracks and also the adhesion of these tracks on the substrate. The geometrical properties are determined by optical image processing and profile analysis. To measure the electrical parameters a micro 4-point probe measuring system is used.*

*Key words: Aerosol Jet® Printing, optimization, interconnects.*

## 1. INTRODUCTION

The production of multifunctional, customized products is getting more and more important these days. Additive Manufacturing (AM) and in particular, the Direct Writing (DW) methods (a subcategory of AM), are very suitable for producing these kind of products. DW techniques have the ability to write or print parts with sub-micron features (e.g. electronic circuits with including conductors, insulators, batteries, antennas, capacitors, etc.) directly from a Computer Aided Design (CAD) file without requiring any pre-processing steps like tooling or mask preparation. This is because DW technologies deposit a material and building a part layer by layer. The AJP process belongs to the droplet-based DW techniques [1], and is based on a carrier gas that provides kinetic energy for the deposition of a material. In our research AJP is used for printing silver interconnects on polyimide substrates. This paper discusses a quantitative method for determination of the process window consisting a set of parameters which will provide good line quality.

## 2. AEROSOL JET PRINTING PROCESS

### 2.1 Advantages of AJP technology

The AJP process was originally developed for manufacturing customised micro-electronics. The process is becoming an alternative for thick-film processes and printing processes, such as screen-, stencil- or inkjet printing. This last technology is the closest related to AJP, although AJP allows smaller print resolution, the deposition of material on non-planar substrates and larger nozzle to substrate distance compared to inkjet. Therefore AJP is generally more flexible than other printing processes and is ideal for manufacturing 3D conformal electronics. [2]

Due to its larger viscosity range (0,7 to 2500 mPa.s) AJP allows the deposition of different ink (or ink-like) materials; e.g.: metal-inks, polymer thick film pastes, diluted ceramic powder or epoxies. [3, 4] [5] Those are the reasons why AJP is becoming a promising technique in the printed electronics industry, with a broad application area including flexible electronics, embedded components (interconnects, resistors, sensors), EMI shielding, flexible displays and solar cells.

## 2.2 Working principle

The principle of aerosol deposition with its process control module (PCM) parameters is shown in Fig. 1. The basic AJP system consists of two important key components: the atomizer and a focussing module in the nozzle. Inks with a viscosity range of 1 to 1000 mPa.s and particle size up to 500 nm can be atomized by a pneumatic atomizer. This type of atomizer uses a high velocity gas stream to generate the aerosol. The aerosol droplets are then transported through the virtual impactor (VI). The ultrasonic atomizer which uses an ultrasonic transducer for generating the aerosol is suited for inks with a viscosity range of 0,7 to 30 mPa.s and small solid particle size of maximum 50 nm. This type of atomizer does not need a VI.

After the aerosol is generated in the atomizer (1) and passes through the VI (2) the print head (3) focuses the aerosol into a concentrated beam by adding a concentric mantle of sheath gas (4) around the aerosol. The focused aerosol stream is directed by the sheath gas to the substrate. By using a sheath gas the aerosolized droplets remain tightly focused over a distance typically from 3 to 5 mm, giving AJP the ability to print over uneven substrates.

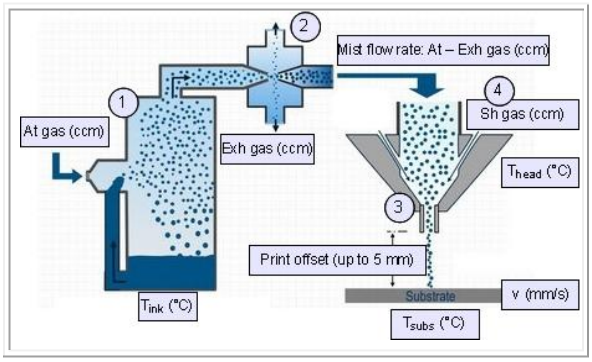

Fig. 1. Aerosol Jet® Printing with pneumatic atomizer [6]

Pre treatment of the substrate include thorough cleaning to reinsure a constant wettability of the deposited material over the entire surface.

## 2.3 Influential parameters of the line width

There are a lot of influence factors which will affect the quality of the printed lines. (see Fig. 2.) In particular, the substrate/ink combination, the process settings of the Aerosol Jet system, the number of layers, as well as the relative speed between substrate and print head are relevant to printing quality. [7]

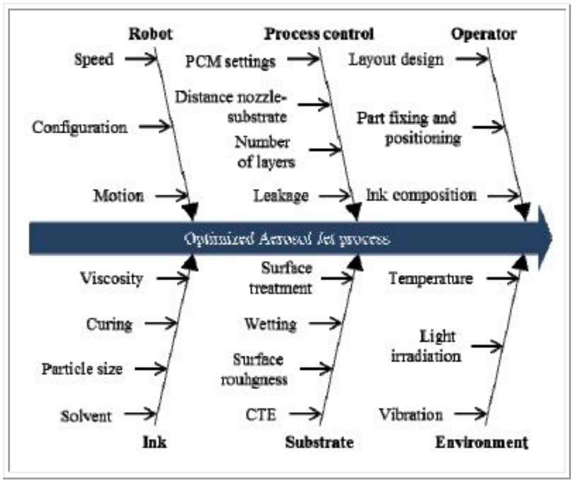

Fig. 2. Factors of influence for the Aerosol Jet® system [7]

The width control of the aerosol beam and thus the line width of the deposited line are controlled by various parameters. The most important PCM parameters are the aerosol gas flow rate, exhaust gas flow rate at the VI, the sheet gas flow rate, the ink temperature and viscosity, the nozzle diameter, the print head temperature and the nozzle to substrate distance (print offset).

The mist flow rate will affect the output rate of material, and thus the line width. The sheath gas flow rate has a smaller influence on the line width. Line width increases with greater print offset. More narrow and higher lines can be obtained by altering the ink formulation (higher viscosity, faster drying , increased surface tension between ink and substrate) or by altering PCM parameters.

A raise of the ink temperature decreases the output rate thus influences the line width. Increasing print head temperature partially dries the aerosol prior to printing, resulting in narrower printed lines. Excessive drying of the aerosol leads to poor print quality (interruption of the printed line) and could eventually block the nozzle. Slightly reducing the mist flow rate in conjunction with heating the print head results in even narrower printed lines. [8]

### 2.4 Influence parameters on overspray

Fig: 5. left shows an example of overspray. This phenomenon is usually caused by the smallest droplets in the aerosol. Overspray can be controlled by adjusting some of the AJP settings such as: the atomization gas flow rate, the sheath gas flow rate and the print offset, or by adjusting the ink formulation. [9] To minimize overspray, flow rates (most importantly atomization flow rate) may not be too high.

Excessive overspray occurs when sheath gas flow rate and print head temperature are set too high. Both will cause excessive drying of the aerosol ink, which will also influence the overspray.

An often underestimated influential parameter on the line quality is the cleaning strategy of the substrate. The surface preparation of the substrate affects the surface tension and thus the wettability. A low surface energy substrate will cause less wetting, which results in a bigger contact angle, changing the topography of the printed lines. (See Fig. 3.)

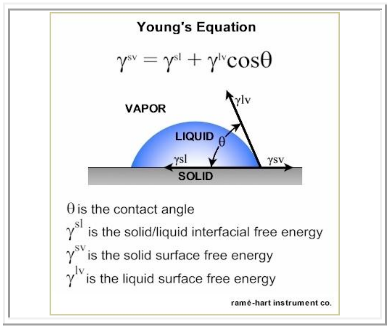

Fig. 3. Contact angle and surface energy [10]

Consistent printing of ink with the Aerosol Jet® System requires a consistent surface, not only because of the proper surface energy of the substrate but also because of the increased possibility for contamination such as oils, fingerprints, dust and atmospheric absorbed materials.

### 2.5 Post-processing of deposited lines

In a post-processing step the deposited lines are sintered, this is almost always carried out to improve the mechanical and electrical properties of the printed material. [11] The choice of sinter temperature and time is based on the ink and substrate. The conductivity of the CSD-32 ink from Cabot, used for our experiments, in function of the sinter temperature during a sinter time of 30 minutes is examined, the results are shown in Fig. 4 [12].

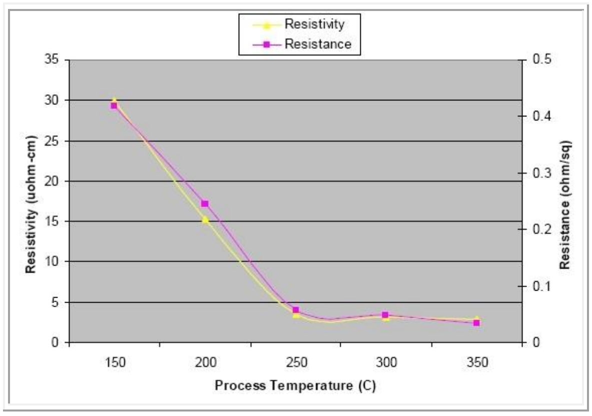

Fig. 4. Electrical properties of Aerosol Jet printed traces on glass, 30min. cure time [12]

## 3. OPTIMIZATION OF AJP FOR SILVER INK

### 3.1 Preliminary research

As explained in paragraphs 2.3 and 2.4 a lot of influence factors determine the printed line width and quality. It is therefore difficult to determine a proper process window which will provide the desired line width and line quality. A preliminary research was set up to have an overview of the process window consisting parameter combinations. A literature review and information of our machine supplier (Optomec®) provided a first set of parameters for performing a preliminary research. Good print results were obtained for atomization flow rates (At gas) of 500 to1000 ccm, mist flow rates of 10 till 25 ccm (atomization minus the exhaust flow rate (Exh gas)), ink temperatures ($T_{ink}$) of 15 to 30 °C, print head temperatures ($T_{head}$) of 20 to 80 °C, print speeds (v) of 1 to 20 mm/s, print offset of 1 to 5 mm, temperatures of the substrate ($T_{subs}$) of 60 to 90 °C and sheath gas flow rates (Sh gas) dependant on the setting of the atomization gas. [13]

The used CSD-32 ink consists of silver nanoparticles (size < 60 nm and wt% of 45-55) with a polymer coating, dispersed in a glycol solvent. This ink was printed onto untreated LCD glass plates with a 150 µm nozzle diameter. (see Table 1)

For each setting five lines where printed.

| **At gas (ccm)** | **Sh gas (ccm)** | **Mist flow (ccm)** |
|---|---|---|
| 550-800 | 20-110 | 20-40 |
| **Nozzle (µm)** | **$T_{subs}$ (°C)** | **Print offset (mm)** |
| 150 | 80 | 3 |
| **Tink (°C)** | **Thead (°C)** | **v (mm/s)** |
| 22-37 | 22-37 | 1-5-10 |

Table 1. PCM parameters of the preliminary research

For the determination of a rough process window for good line quality, three images of every five lines were taken with the alignment camera and a general quality attribute from 1 to 10 was given to these images. (see Table 2) An example of a few quality attributes are given in Fig. 5.

| | |
|---|---|
| 1 | bad, no adhesion |
| 2 | bad, big droplets |
| 3 | moderate, enough adhesion |
| 4 | moderate, less big droplets |
| 5 | moderate, overspray |
| 6 | moderate, too fluent (wavy) |
| 7 | moderate, stains/discontinuous |
| 8 | good, soft stains |
| 9 | good, too fine |
| 10 | good, fine (edge!) |

Table 2. General quality attributes

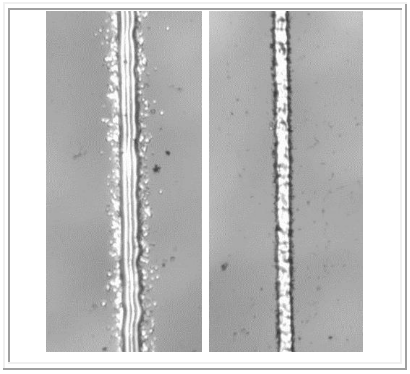

Fig. 5. Examples quality attribute 5-moderate (left) and 10-good (right)

This rough line quality determination gave a first impression of the process window.(see Fig. 6.) Although this process window is quite broad, it provided a good starting point for the set-up of further qualitative analysis and process optimization.

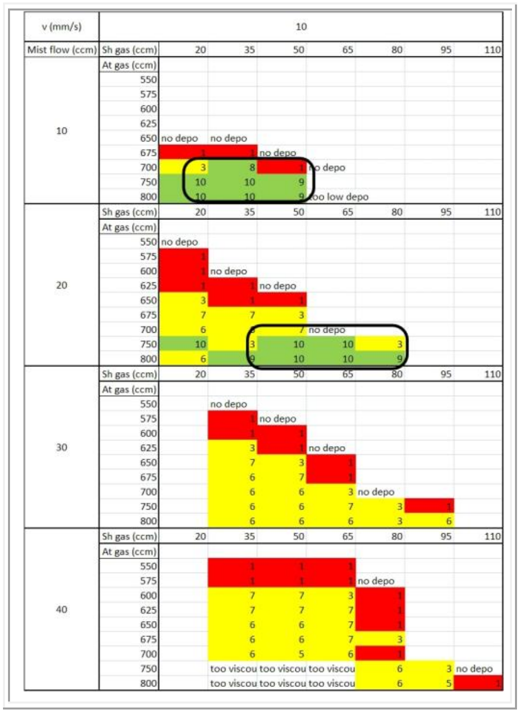

| v (mm/s) | | 10 | | | | | | |
|---|---|---|---|---|---|---|---|---|
| Mist flow (ccm) | Sh gas (ccm) | 20 | 35 | 50 | 65 | 80 | 95 | 110 |
| 10 | At gas (ccm) | | | | | | | |
| | 550 | | | | | | | |
| | 575 | | | | | | | |
| | 600 | | | | | | | |
| | 625 | | | | | | | |
| | 650 | no depo | no depo | | | | | |
| | 675 | 1 | 1 | no depo | | | | |
| | 700 | 3 | 8 | 1 | no depo | | | |
| | 750 | 10 | 10 | 9 | | | | |
| | 800 | 10 | 10 | 9 | too low depo | | | |
| 20 | Sh gas (ccm) | 20 | 35 | 50 | 65 | 80 | 95 | 110 |
| | At gas (ccm) | | | | | | | |
| | 550 | no depo | | | | | | |
| | 575 | 1 | | | | | | |
| | 600 | 1 | no depo | | | | | |
| | 625 | 1 | 1 | no depo | | | | |
| | 650 | 3 | 1 | 1 | | | | |
| | 675 | 7 | 7 | 3 | | | | |
| | 700 | 6 | 6 | 7 | no depo | | | |
| | 750 | 10 | 3 | 10 | 10 | 3 | | |
| | 800 | 6 | 9 | 10 | 10 | 9 | | |
| 30 | Sh gas (ccm) | 20 | 35 | 50 | 65 | 80 | 95 | 110 |
| | At gas (ccm) | | | | | | | |
| | 550 | | no depo | | | | | |
| | 575 | | 1 | no depo | | | | |
| | 600 | | 1 | 1 | | | | |
| | 625 | | 3 | 1 | no depo | | | |
| | 650 | | 7 | 3 | 1 | | | |
| | 675 | | 6 | 7 | 1 | | | |
| | 700 | | 6 | 6 | 3 | no depo | | |
| | 750 | | 6 | 6 | 7 | 3 | 1 | |
| | 800 | | 6 | 6 | 6 | 3 | 6 | |
| 40 | Sh gas (ccm) | 20 | 35 | 50 | 65 | 80 | 95 | 110 |
| | At gas (ccm) | | | | | | | |
| | 550 | | 1 | 1 | 1 | | | |
| | 575 | | 1 | 1 | 1 | no depo | | |
| | 600 | | 7 | 7 | 3 | 1 | | |
| | 625 | | 7 | 7 | 7 | 1 | | |
| | 650 | | 6 | 6 | 7 | 1 | | |
| | 675 | | 6 | 6 | 7 | 3 | | |
| | 700 | | 6 | 5 | 6 | 1 | | |
| | 750 | | too viscou | too viscou | too viscou | 6 | 3 | no depo |
| | 800 | | too viscou | too viscou | too viscou | 6 | 5 | 1 |

Fig. 6. Rough line quality determination of a broad PCM parameters range

### 3.1 Preliminary tests for resistivity and profile analysis

Besides the determination of line quality, the resistivity and cross section of the printed lines has to be defined for electrical property quantification.

Electrical resistivity measurements were performed with a micro-4-point-probe (M4PP). For these measurements a circuit was designed. (see Fig. 7.)

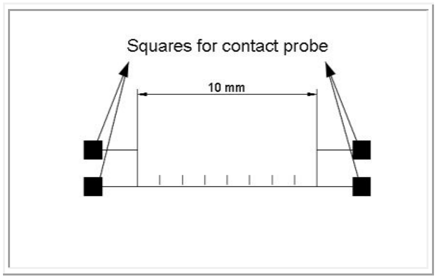

Fig. 7. Circuit for printing and measuring with M4PP

The circuit was printed with CSD-32 ink (also used in the previous tests) on glass which was treated with aceton for 10 min. at 40 °C, and then cleaned with IPA sonication for 5 min.. Because the contact probes of the M4PP damaged the printed silver ink squares, our M4PP system was not suited for measuring these samples. Samples printed on polyimide tape would give better adhesion and resistance measurements could be performed. The set-up PCM parameters for samples printed on polyimide are given in Fig. 8. top. The polyimide tape was attached to a glass plate to provide a flat surface, and was treated with the same cleaning strategy as the previous experiment. Using a micro profile tracker the cross section of the printed lines was measured. (see Fig. 8. bottom) The best sample had a calculated resistivity of 72 μΩ-cm.

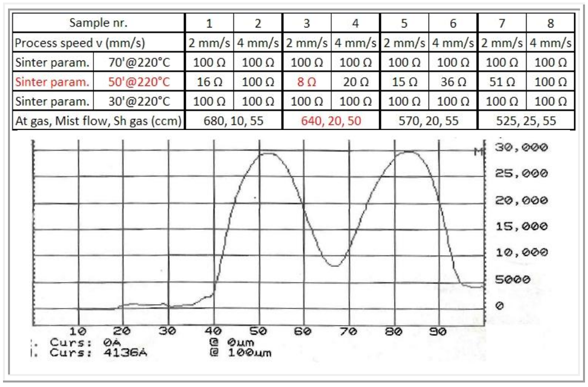

| Sample nr. | | 1 | 2 | 3 | 4 | 5 | 6 | 7 | 8 |
|---|---|---|---|---|---|---|---|---|---|
| Process speed v (mm/s) | | 2 mm/s | 4 mm/s | 2 mm/s | 4 mm/s | 2 mm/s | 4 mm/s | 2 mm/s | 4 mm/s |
| Sinter param. | 70'@220°C | 100 Ω | 100 Ω | 100 Ω | 100 Ω | 100 Ω | 100 Ω | 100 Ω | 100 Ω |
| Sinter param. | 50'@220°C | 16 Ω | 100 Ω | 8 Ω | 20 Ω | 15 Ω | 36 Ω | 51 Ω | 100 Ω |
| Sinter param. | 30'@220°C | 100 Ω | 100 Ω | 100 Ω | 100 Ω | 100 Ω | 100 Ω | 100 Ω | 100 Ω |
| At gas, Mist flow, Sh gas (ccm) | | 680, 10, 55 | | 640, 20, 50 | | 570, 20, 55 | | 525, 25, 55 | |

Fig. 8. Ω/10mm values per PCM parameter (top); profile of best sample of 8 Ω/10mm (bottom)

According to Cabot's datasheet the expected resistivity value for this ink is normally ten times less. (see Fig. 4.) The quality analysis using quality attributes 1 to 10 based on pictures taken with the alignment camera appeared to be insufficient for determining a good process window. A more profound analysis was therefore needed.

### 3.1 Quantitative analysis with vision based 2D quality control

The preliminary research using an analysis based on quality attributes gave a broad range of parameter combinations. Therefore succeeding research was needed. This research started from the best PCM parameters selected in the preliminary research and new samples were printed with these settings. Five lines of 10 mm were printed for each PCM setting and every 3 mm an image of ±0,5 mm² was taken along each line. A more profound 2D quality control for quantitative analysis was then set-up.

The line width, the overspray and satellite droplet detection and smoothness of the track were measured on these images. An own-written edge detection algorithm was used to automatically detect zones. (see Fig. 9.)

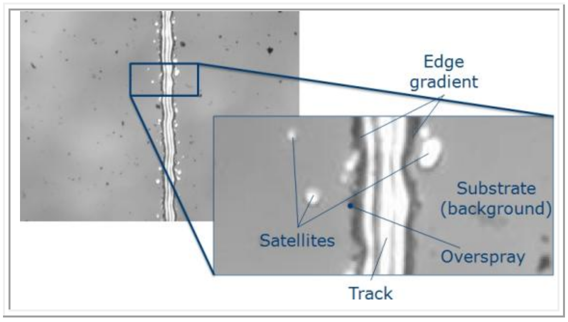

Fig. 9. Different zones of edge detection using maximum gradient greyvalue

Defining the track edges was a first step towards analyzing the track. Based on this data, the line width of the track could be calculated and an analysis of the edge could be made. The different steps consisted of reducing the search zone for the edge, using the gradient of edge as a start position of search and finding the left and right edge based on maximum gradient principle.(see Fig.10).

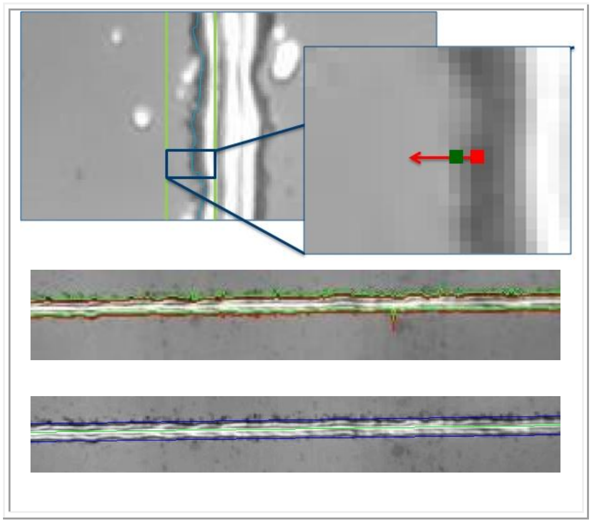

Fig. 10. Gradient of edge (top); samples of edge detection algorithm (bottom)

The line width determination was performed by fitting (Gaussian) a line through the left and right edge. The symmetric line was then calculated and the mean distance left and right to the symmetric line was calculated.

The track edge smoothness was defined by fitting a line through both left and right edge. The smoothness of the edge was calculated by using the shortest distances between edge and fitted line. (equation 1)

$$Es_a = \frac{1}{L}\sum_{i=1}^{n}|z_i| \qquad (1)$$

In equation (1) the shortest distances to the fitted line are represented by $z$. The total length of the line is represented by $L$. The calculated edge smoothness is represented by $Es_a$.

Faulty measurement sometimes occurred but these pictures and extreme data were filtered out manually. An edge detection fault can occur, the bulging effect can influence the line width measurement and the edge determination is sometimes not optimally separated from the overspray zone.

## 4. DETERMINATION OF THE DETAILED PROCESS WINDOW

For determination of the process window, line width and edge smoothness is used. The line width of the printed lines and relative edge smoothness (the smoothness of the edge divided by the line width in µm) are plotted in a 3D scatter graph using the AJP gas flow rates in the X, Y and Z axis. The line width is represented by the size of the sphere were a tenth of the nozzle's diameter is the nominal value and smallest sphere size. The relative edge smoothness is represented by a colour compared to the colour legend. (see Fig. 11.)

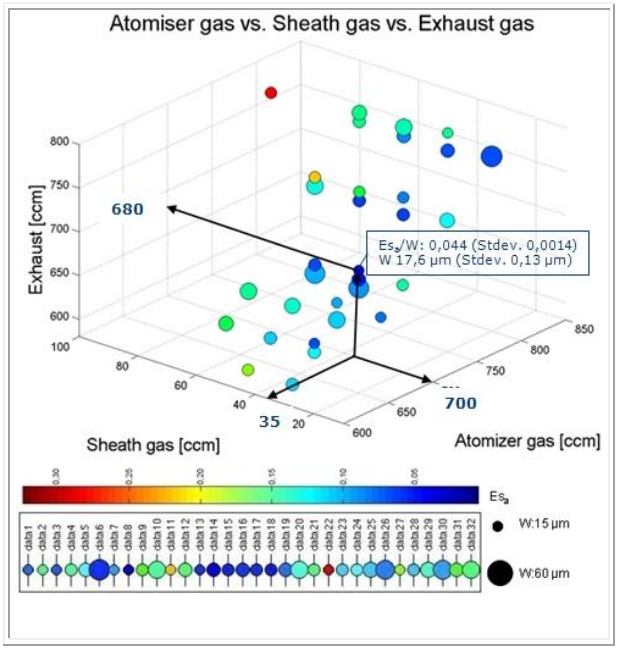

Fig. 11. 3D scatter graph with as best result Es$_a$/W of 0,044 (Stdev. 0,0014) and W of 17,6 µm (Stdev. 0,13 µm)

The results with the smallest line width (17,6µm) and best relative edge smoothness (0,044) seemed to be also the best line quality of all the printed silver lines. The PCM parameters were: At gas of 700 ccm, Exh gas of 680 ccm and a Sh gas of 35 ccm. The parameter combination for optimal quality can thereby be selected using this edge detection algorithm for further optimization of the AJP process.

## 5. FUTURE WORK

Further optimization of AJP silver ink lines will be done for better determination of the process window. A profile analysis and resistivity measurement will be done of printed samples with PCM parameters of the optimized zone in the 3D graph.
Future research work concerning the algorithm will be set-up to put more intelligence in the edge determination. Other important quality attributes are track interruption, bulging and zone detection within a track.

## 6. CONCLUSION

After a preliminary research using a rough quality control method based on images, a more profound research was set up to determine the parameter combination for optimal quality. The glass substrate was replaced by polyimide tape to improve attachment and different characteristics of the printed lines were measured and used to setup a quality analysis tool. The line width and smoothness of the edge are measured with the aid of a vision system. Based on these measurements a 3D scatter plot is generated and used for determining a process window where good line quality is achieved, further optimization is still required.

## ACKNOWLEDGEMENTS

The authors acknowledge the support of the IWT in the framework of the EraSME 3DAMEEA project PO7810-EUR-ERA-01

## 7. REFERENCES

[1] Hon, K.K.B., Li, L. and Hutchings, I.M. Direct writing technology—Advances and developments. *Annals of the CIRP-Manufacturing Technology,* 2008, **57**, 601-620.
[2] Watson, S. Aerosol Jet® Printed Electronics Overview, New Mexico (Albuquerque) USA, [WWW] http://www.optomec.com (02.03.2012)
[3] Hedges, M. 3D MID Manufacture via the M3D Process. In *Proceedings of the 8th International Congress Molded Interconnect Devices,* Nuremberg Fuerth, Germany, September 24.-25. 2008.
[4] Akedo, J. Microstructure of ceramic thick film formed by aerosol deposition and its applications to microactuator. *Integr. Ferroelectr.* ,2006, **1**, 55-65.
[5] Brose, M. et al. Aerosol Deposition of Catalytic Ink to Fabricate Fine Pitch Metallizations for Moulded Interconnect Devices (MID). In *Electronic System Integration Technology Conference (ESTC),* 2010, 1-4.
[6] Folgar, C.E. et al. Solution-based aerosol deposition process for synthesis of multilayer structures. *Materials Letters*, 2011, **65**, 1302-1307.
[7] Goth, C., Putzo, S., Franke,J. Aerosol Jet Printing on Rapid Prototyping Materials for Fine Pitch Electronic Applications. In *Electronic Components and Technology Conference (ECTC),* 2011, 1211-1216.
[8] King, B.H. et al, Characterizing Aerosol Jet® Multi-Nozzle Process Parameters for Non-Contact Front Side Metallization of Silicon Solar Cells. In: *Photovoltaic Specialists Conference (PVSC)*, 34th IEEE, 2009.
[9] Grunwald, I. et al. Surface biofunctionalization and production of miniaturized sensor structures using aerosol printing technologies. Biofabrication, 2010, **2,** 014106.
[10]Contact angle [WWW] http://www.ramehart.com/contactangle.htm (02.03.2012)
[11] O'Reilly, M and Leal, J. Jetting Your Way to Fine-pitch 3D Interconnects. In: *Chip Scale Review*[online], September-October 2010, 18-21.
[12] Cabot Printed Electronics Materials, Datasheet CSD-32 Cabot Fine Particle Silver Ink.
[13] Optomec Inc. Aerosol Jet Deposition System Manual, Albuquerque, 2010.

## CONTACT

**Ing. Wesley Verheecke MEng. - Manufacturing Engineering**
Lessius Mechelen University College | Campus De Nayer
Faculty of Industrial Engineering Sciences – Manufacturing Engineering (K.U.Leuven Association)
Jan De Nayerlaan 5 | 2860 Sint-Katelijne-Waver | Belgium
Tel + 32 15 31 69 44 | Fax + 32 15 31 74 53
wesley.verheecke@lessius.eu